Detection and Diagnosis of Ring Formation in Rotary Lime Kilns

Authors:

Lee D Rippon, Barry Hirtz, Carl Sheehan, Travis Reinheimer, Cilius van der Merwe, Philip Loewen, Bhushan Gopaluni

Date Submitted: 2021-10-21

Keywords: process monitoring, Fault Detection, fault diagnosis, data visualization, pulp and paper, rotary kiln

Abstract:

Rotary lime kilns are large-scale, energy-intensive unit operations that serve critical functions in a variety of industrial processes including cement production, pyrometallurgy, and kraft pulping. As massive expensive vessels that operate at high temperatures it is imperative from economic, environmental, and safety perspectives to optimize preventative maintenance and production efficiency. To achieve these objectives rotary kilns are increasingly outfitted with more sophisticated sensing technology that can provide additional operating insights. Although increasingly intricate data is collected from industrial operations the extent to which value is extracted from this data is often far from optimal. Our research aims to improve this situation by developing data analytics methods that leverage advanced industrial sensor data to address outstanding process faults. Specifically, this research investigates the use of infrared thermal cameras to detect and diagnose ring formation in rotary lime kilns. The formation of rings is described in literature as the most troublesome problem for lime kiln operation as it can severely limit production, cause millions of dollars in equipment damage, and lead to unplanned shutdowns. In this work we propose a strategy to detect and diagnose ring formation with industrial thermal camera data. While implementing this strategy with an industrial case study we develop a novel process visualization technique and obtain important process insights that enable better data collection. These contributions are presented in this work along with preliminary results from ring detection and diagnosis, on-going challenges, and suggestions for future research directions.

Record Type: Published Article

Submitted To: LAPSE (Living Archive for Process Systems Engineering)

Citation (overall record, always the latest version):	LAPSE:2021.0792
Citation (this specific file, latest version):	LAPSE:2021.0792-1
Citation (this specific file, this version):	LAPSE:2021.0792-1v1

CSChE Systems & Control Transactions

Open Access | Original Research

Conference Proceedings
Canadian Chemical Engineering Conference 2021
October 24-27, Montréal, Québec, Canada

PSEcommunity.org/LAPSE:2021.0792

PSE PRESS

Detection and Diagnosis of Ring Formation in Rotary Lime Kilns

Lee D. Rippon[a]*, Barry Hirtz[b], Carl Sheehan[c], Travis Reinheimer[d], Cilius van der Merwe[d], Philip Loewen[e], and Bhushan Gopaluni[a]

[a] University of British Columbia, Department of Chemical and Biological Engineering, Vancouver, B.C., Canada
[b] Cool Cameras, Prince George, B.C., Canada
[c] Spartan Controls, Burnaby, B.C., Canada
[d] Canfor Pulp, Vancouver, B.C., Canada
[e] University of British Columbia, Department of Mathematics, Vancouver, B.C., Canada
* Corresponding Author: leeripp@chbe.ubc.ca

ABSTRACT

Rotary lime kilns are large-scale, energy-intensive unit operations that serve critical functions in a variety of industrial processes including cement production, pyrometallurgy, and kraft pulping. As massive expensive vessels that operate at high temperatures it is imperative from economic, environmental, and safety perspectives to optimize preventative maintenance and production efficiency. To achieve these objectives rotary kilns are increasingly outfitted with more sophisticated sensing technology that can provide additional operating insights. Although increasingly intricate data is collected from industrial operations the extent to which value is extracted from this data is often far from optimal. Our research aims to improve this situation by developing data analytics methods that leverage advanced industrial sensor data to address outstanding process faults. Specifically, this research investigates the use of infrared thermal cameras to detect and diagnose ring formation in rotary lime kilns. The formation of rings is described in literature as the most troublesome problem for lime kiln operation as it can severely limit production, cause millions of dollars in equipment damage, and lead to unplanned shutdowns. In this work we propose a strategy to detect and diagnose ring formation with industrial thermal camera data. While implementing this strategy with an industrial case study we develop a novel process visualization technique and obtain important process insights that enable better data collection. These contributions are presented in this work along with preliminary results from ring detection and diagnosis, ongoing challenges, and suggestions for future research directions.

Keywords: process monitoring, fault detection and diagnosis, data visualization, pulp and paper, rotary kiln

Date Record: Original manuscript received October 18, 2021. Published October 21, 2021

INTRODUCTION

As the digital transformation of industrial processes progresses it becomes increasingly important to develop application specific data analytics techniques that maximize the value extracted from process data. The global emergence of digitalization has placed data in a central role in modern society. The vital role of data has drawn increased attention to data analytics fields such as artificial intelligence, machine learning, and process systems engineering. This increased attention has manifested in process monitoring literature in the form of increasingly sophisticated fault detection and diagnosis algorithms. From traditional techniques such as principal component analysis (PCA) to advanced deep learning architectures such as generative adversarial networks (GANs), new state-of-the-art results are frequently published on popular simulated benchmarks such as the Tennessee Eastman process [1,2]. Unfortunately, in many industries the advances in process monitoring algorithms have not necessarily translated to increased uptake and successful implementation.

This research aims to develop and apply data analytics techniques to address a specific outstanding industrial fault, i.e., ring formation in rotary lime kilns. Ring formation is a significant industrial fault that contributes to immense economic and environmental losses. It deserves and has received attention in literature [3-5], but it has not received significant attention from the relevant data analytics communities, e.g., process monitoring [6]. By centering our data-driven investigation around a specific fault with real historical data we must directly address many of the practical constraints and implementation challenges. Fortunately, these challenges also provide opportunities to develop techniques for learning valuable process insights from the often-undervalued raw data [7].

In this paper we present the findings of our investigation into using historical process data to detect and diagnose ring formation in a rotary lime kiln. After providing process knowledge for context, we present our proposed approach for detecting and diagnosing ring formation. Data visualization and monitoring tools are developed to enhance our

investigation and obtain valuable process insights. Preliminary results reveal unique challenges associated with ring detection which inform enhanced data collection techniques and opportunities for future research.

BACKGROUND

The process monitoring techniques presented in this work are relevant to a variety of industries where rotary kilns collect real-time kiln shell temperature (KST) measurements along the length of the kiln. However, investigating ring formation requires specific domain knowledge so the remainder of this work will focus on a particular application, i.e., rotary lime kilns in the recovery circuit of kraft pulp mills. The rest of this section provides context into the role of the lime kiln in the recovery circuit, describes the problem of ring formation, and presents the available resources to help set the stage for our investigation.

Kraft Pulping and Rotary Lime Kilns

As Figure 1 illustrates, rotary lime kilns (outlined in red) are part of the larger integrated forest products industry. Pulp mills are a key component of the integrated forest products industry as the profitability of sawmills depends on revenue generated through selling chips to pulp mills [8]. The kraft pulping process relies upon a strong alkaline solution known as white liquor. Kraft pulp mills also rely on a recovery circuit to recover expensive chemicals (e.g., white liquor) and minimize their environmental impact. Central to chemical recovery is the recausticizing area which produces white liquor by reacting green liquor with slaked lime. This causticizing reaction produces lime mud as a by-product. The rotary lime kiln is essential for regenerating burnt lime from this lime mud [9].

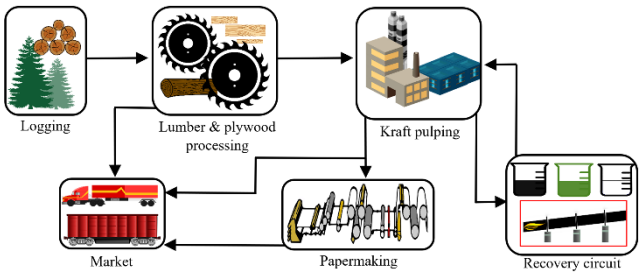

Figure 1. The role of the lime kiln (outlined in red) in the context of the integrated forest products industry.

Rotary lime kilns are massive cylindrical vessels consisting of a slightly inclined steel shell that can be over 100 m in length and over 4 m in diameter [10]. The steel shell is lined with protective refractory bricks, supported by external bracing, and rotated by a drive gear at roughly 1 rpm [9]. The kiln is responsible for converting calcium carbonate ($CaCO_3$) into calcium oxide (CaO) according to the following endothermic calcination reaction:

$$CaCO_3(s) \rightarrow CaO(s) + CO_2(g). \quad (1)$$

The calcination reaction proceeds at roughly 870°C [3]. As Figure 2 illustrates, wet lime mud ($CaCO_3$) enters the lime kiln where it dries into a powder in the drying zone before agglomerating into nodules in the preheating zone. The energy required for drying, preheating, and calcining the lime mud is provided by a burner flame at the bottom of the inclined shell. The burner often uses natural gas and is the largest source of fuel consumption in pulp manufacturing [11]. Given the high fuel demand and the nature of calcination the lime kiln is a very carbon intensive unit operation so there is a strong environmental motivation for minimizing production inefficiencies.

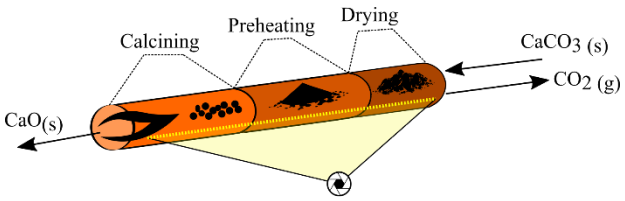

Figure 2. Simplified illustration of a rotary lime kiln with a thermal camera measuring shell temperatures.

Another detail illustrated in Figure 2 is the use of a thermal camera to provide real-time KST measurements along the length of the kiln. As thermal imaging technology has matured it has become less expensive while offering better performance and functionality. Consequently, kilns have become increasingly equipped with infrared cameras which are primarily used to monitor shell temperatures for potentially dangerous hot spots [12]. As more kilns are equipped with thermal cameras it becomes increasingly important to maximize the value extracted from this supplementary data. This work aims to leverage this data to address a major outstanding process fault that many kilns suffer from, i.e., the formation of rings.

Kiln Fouling and Ring Formation

Reaction materials flow through the kiln because of the slope and rotation speed of the kiln. Apart from a thin coating that is applied to the refractory during start-ups there should be no accumulation of material in the kiln. Fouling occurs when reaction material accumulates in the kiln. Two distinct types of fouling are shown in Figure 3, i.e., soda balls (left) and rings (right). Ring formation has been described in literature as the most troublesome problem for lime kiln operation [13]. Rings form when lime mud and product lime particles adhere to the refractory wall of the kiln and begin to accumulate. Although the exact mechanisms of ring formation are not completely understood, distinct types of rings have been observed and causal mechanisms have been proposed [3].

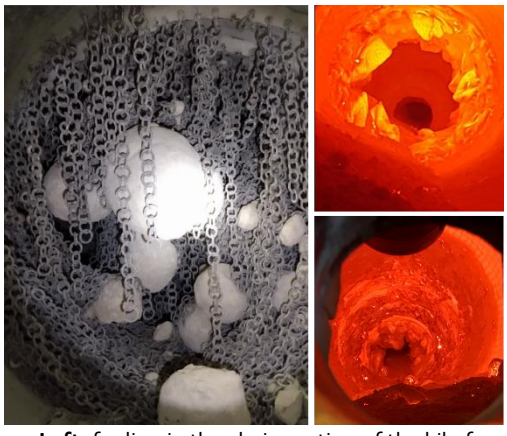

Figure 3. Left: fouling in the chain section of the kiln from soda balls. **Right:** two distinct cases of ring formation.

A survey of Swedish kraft pulp mills showed that approximately 70% of mills suffered from ring formation and many did not know why [14]. As rings grow, they can obstruct the flow of reaction materials in the kiln which can result in reduced production of lime. To compensate for this lost production mills must purchase fresh lime which can cost over $50,000 USD per day. In severe cases the rings can result in damage to the kiln refractory which can cost over $3 million USD per event [3]. Perhaps the costliest consequence of ring formation is that it can regularly lead to unscheduled downtime. Mills attempt to mitigate ring formation by using industrial shotguns to blast out the ring, thermal cycling to cause stress fractures, and adding water to the kiln to slake out the ring. These temporary measures can help prolong operation of a fouled kiln, but ultimately a full shut-down is typically required for someone to enter the kiln and use a pneumatic jack hammer to physically remove the ring.

Objectives and Available Resources

The objectives of this work are two-fold:

1. **Detect ring formation:** early onset detection of ring growth and decay. Estimating the extent and rate of ring formation to enable preventative maintenance and avoid refractory damage.
2. **Diagnose potential causes:** analyze process data to identify significant associations between ring formation and operating conditions. Determine improved operating policies that can extend the time between unplanned shutdowns.

Historical process data from a lime kiln with known fouling problems is the primary resource available to achieve these objectives. Hourly averaged samples over five years of operation are taken from the process historian. The data includes over sixty relevant process variables (PVs) (e.g., firing rates, feed rates, moisture content, etc.) of which thirty are from three different thermal cameras. Raw thermal camera images, such as the one shown in Figure 4, are available at four-hour intervals. The KST profile is constructed from twenty-four measurement areas, such as those shown in Figure 4. Each of the three thermal cameras provides ten measurements; eight measurement areas for the KST profile and two measurements related to exterior bracing. Communications with engineers and a mill personnel is another important resource.

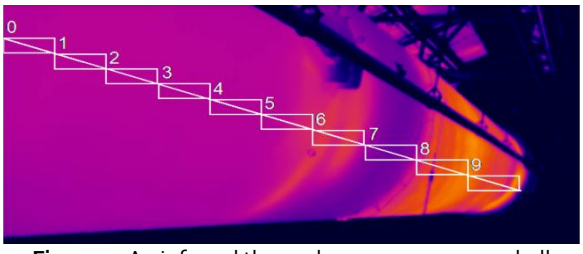

Figure 4. An infrared thermal camera measures shell temperatures along the length of a rotary lime kiln [7].

METHODOLOGY

In this section we describe the proposed methodology for using the available resources to accomplish our ring detection and diagnosis objectives. First, specific strategies for detection and diagnosis are presented. This is followed by a description of our novel approach to process visualization which is instrumental to our ongoing investigations.

Detecting and Diagnosing Ring Growth

In literature fault detection is often reduced to binary classification, i.e., whether or not a fault has occurred. Likewise, diagnosis is often reduced to multi-class classification, i.e., which fault occurred. These experiments are dependent on idealistic labelled datasets where there is no ambiguity regarding the ground-truth of the class labels [15]. In practice, when dealing with outstanding industrial faults and real historical process data, the situation is often far less ideal. In our case, there is no labelled dataset that says where and when faults occurred and what the exact cause was. Instead, as we discuss in what follows, most of the work involves developing techniques to reliably label the historical data.

Residual monitoring and ring detection

The primary objective of ring detection is to provide early indications of ring formation so corrective actions can be taken by operators. A secondary objective of ring detection is to label five years of historical data such that supervised learning methods can be used for identifying high-risk operating conditions and diagnosing ring formation. To accomplish both objectives we develop a validated ring detection algorithm that can automatically identify rings (and therefore provide labels) with new process data.

The proposed ring detection algorithm is based on monitoring residuals (e) between estimated temperatures ($\hat{T}$) and observed temperatures (T). Consider a sample time t as an element of a sequence of sample times $\boldsymbol{t} = (t_1, \cdots, t, \cdots, t_\tau)$ and a specific position x along the KST profile $\boldsymbol{x} = (x_1, \cdots, x, \cdots, x_N)$ measured in terms of distance from the firing end of the kiln. The residual is computed as follows:

$$e(x,t) = \hat{T}(x,t) - T(x,t), \tag{2}$$

where high positive values of the residual indicate a lower-than-expected measured temperature (i.e., potential ring growth), and high negative values indicate a higher-than-expected measured temperature (i.e., potential ring decay). Attributing these residuals to ring formation assumes the mismatch between estimated and actual temperatures is entirely due to rings causing changes in the thermal resistance of the kiln shell wall. The presence of confounding variables (e.g., refractory wear) and disturbances (e.g., measurement noise) make this a precarious assumption. Therefore, to help control for these factors, special consideration must be given to preparing the data and generating temperature estimates.

Two distinct approaches to developing the residual are considered: i) a simple algebraic approach based on a reference start-up profile and *a priori* process knowledge, and ii) an approach based on statistical forecasting. For this work we elaborate on the second approach. Consider a model where the endogenous response variable, $T(t)$, is a vector of the entire KST profile at time t, i.e., $\boldsymbol{T}(t) = (T(x_1,t), T(x_2,t), \cdots, T(x_N,t))^T$. Furthermore, consider a model with variable auto-regressive (AR) order (p), a moving-average (MA) component of variable order (q), and exogeneous regressors (e.g., natural gas feed, mud feed, etc.). This is known as a VARMAX(p,q) model and it models the KST profile at time t as

$$\boldsymbol{T}(t) = \boldsymbol{\varphi_0} + \sum_{i=1}^{p} \boldsymbol{\Phi}_i \boldsymbol{T}(t-i) + \sum_{i=1}^{q} \boldsymbol{\theta}_i \boldsymbol{\varepsilon}(t-i) + \sum_{i=0}^{b-1} \boldsymbol{B}_i \boldsymbol{X}(t-i) + \boldsymbol{\varepsilon}(t), \quad (3)$$

where $\boldsymbol{\varphi_0}$ is a vector of unknown constants, $\boldsymbol{\Phi}_i$ is a matrix of AR coefficients, $\boldsymbol{\theta}_i$ is a matrix of MA coefficients, $\boldsymbol{B}_i$ is a matrix of exogeneous coefficients, and $\boldsymbol{\varepsilon}$ is a vector of error terms. Models of this nature are trained on the historical KST data and temperature forecasts are generated with a rolling origin as demonstrated by Figure 5 below.

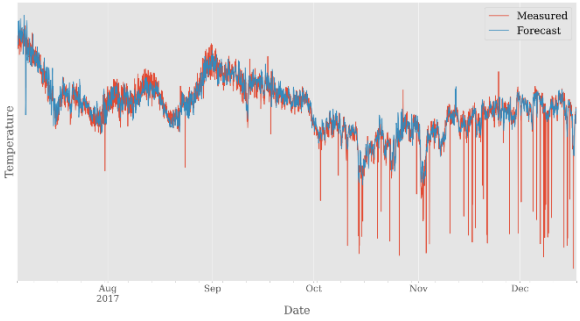

Figure 5. Statistical forecasting of kiln shell temperatures.

Taking the difference of the forecasted and measured temperatures results in a series of residuals. The large drops in measured temperature in Figure 5 demonstrate a problem with the raw camera data, i.e., intermittent obstructions of the camera as shown in Figure 6. Therefore, the series of re siduals requires further processing before it can serve as a ring indicator. A simple thresholding strategy is used to extract residuals that are considered significant.

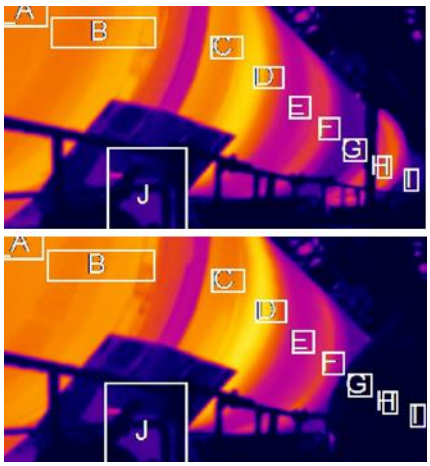

Figure 6. Obstruction of measurement areas G, H and I in the bottom image can corrupt raw data.

Each series of residuals is analyzed as a distribution and the thresholds are based on the first quartile (Q_1), the third quartile (Q_3), and the interquartile range (IQR). Growth residuals, $G(e)$, are extracted as: $Q3 + IQR \leq G(e) \leq Q3 + 3IQR$. Likewise, decay residuals, $D(e)$, are extracted as: $Q1 - 3IQR \leq D(e) \leq Q1 - IQR$. After the significant growth and decay residuals are sampled, daily counts for each growth and decay residual are generated as shown in Figure 7. A final threshold is applied to the daily counts to identify days where ring formation is suspected. Days that are flagged for ring formation are validated with raw data.

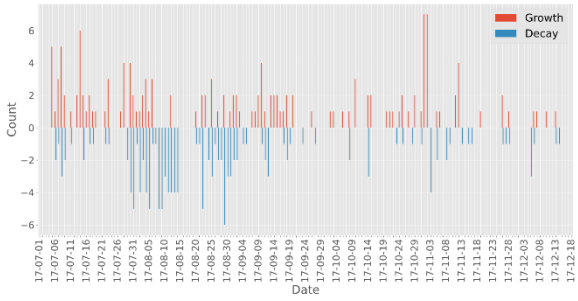

Figure 7. Daily counts for growth and decay residuals.

Supervised learning and ring diagnosis

Once a ring formation indicator has been developed and validated it can be integrated into the historical dataset as a proxy for changes to the state of the ring. Statistical measures, such as cross-correlation with relevant lags, can be quantified to discover significant associations between the ring indicator and relevant PVs. Granger causality tests can be used to determine whether PVs contain information that can help predict ring formation. For non-linear relationships non-parametric statistics such as transfer entropy can be used to quantify transfer of information. Moreover, supervised learning regression models can take PVs as inputs to predict the residuals. If predictions are sufficiently accurate and reliable the models can be interrogated to determine the influence of PVs on ring formation.

As mentioned before, an important prerequisite for using supervised learning to infer causes of ring formation is an accurately labelled dataset. The primary quantitative results in this work involve validating and improving the reliability of ring detection. To supplement for the lack of a high-quality labelled dataset, qualitative insights on diagnosis from research and exploratory data analysis are provided. The exploratory data analysis is enhanced by a novel approach to process visualization as the following subsection describes.

Kiln Monitoring with Interactive Visualization

To detect rings the KST profile needs to be visualized over varying periods of time. A common approach in industry is to overlay KST profiles taken from different periods of interest as demonstrated by the three KST profiles in Figure 8. While this approach to visualizing shell temperatures does

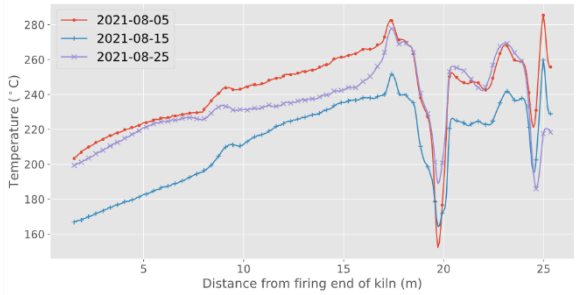

Figure 8. Observing changes in shell temperature profiles by overlaying profiles from ten-day intervals.

provide some insights into KST profile changes over time it is significantly limited. If too few profiles are overlayed, it is uninformative; if too many profiles are overlayed, it is incomprehensible.

To intuitively visualize large quantities of KST profiles in a user-friendly manner we propose the novel visualization strategy presented in Figure 9. This spatiotemporal heatmap shows axial shell temperature variations along the y-axis and continuous temporal shell temperature variations along the x-axis. The y-axis temperatures from Figure 8 are embedded as the uniform, sequential colormap on the right side of Figure 9. Embedding the temperatures as colors enables a clear, intuitive visualization of large quantities of KST data. Previous work demonstrates how the spatiotemporal heatmap is complemented by interactive features to enable visualization of rings over varying timescales and in the context of relevant PVs [7]. This visualization tool has been critical for validating ring detection and exploring the historical data with subject matter experts to extract insights into diagnosis.

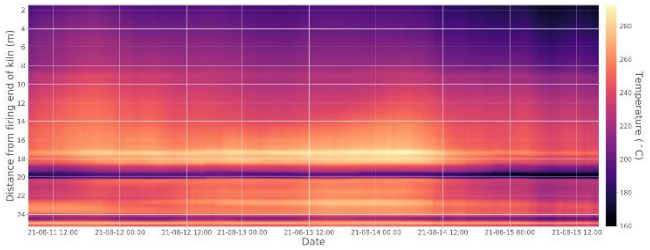

Figure 9. Spatiotemporal heatmap of KST profiles.

RESULTS

The results presented here primarily highlight the efforts made to validate the ring formation indicator. Preliminary insights from manual investigations into ring diagnosis are also presented.

Validating the Ring Formation Indicator

The analysis begins with five years of raw thermal camera data, as shown in the top part of Figure 10. This data contains unwanted data from shutdowns (i.e., black vertical streaks) and sensor failures (i.e., periods with zero variability). The middle plot in Figure 10 shows the result of removing this unwanted data. Extracting periods where the entire KST profile is valid for at least 30 days results in the twelve distinct periods of operation, referred to as experimental trials, shown in the bottom plot of Figure 10.

Although there are 24 measurement positions along the KST profile, for now let us consider just a single position, i.e., 18 m from the firing end of the kiln. A univariate formulation of equation 3 is used to forecast shell temperatures at the 18 m position. The IQR filtering is conducted to sample significant residuals from which daily counts are generated. Figure 5 and Figure 7 demonstrate the forecast and the daily counts at 18 m for the longest experimental trial (i.e., the fifth). This procedure is repeated for each of the twelve experimental trials and a threshold is applied to all 751 days. Days with growth/decay counts greater than 4 are flagged for ring growth/decay, respectively. Ultimately, 24 days are flagged for ring growth and 51 days are flagged for ring decay. Manual validation is conducted for both growth and decay using the raw thermal camera images and other available resources.

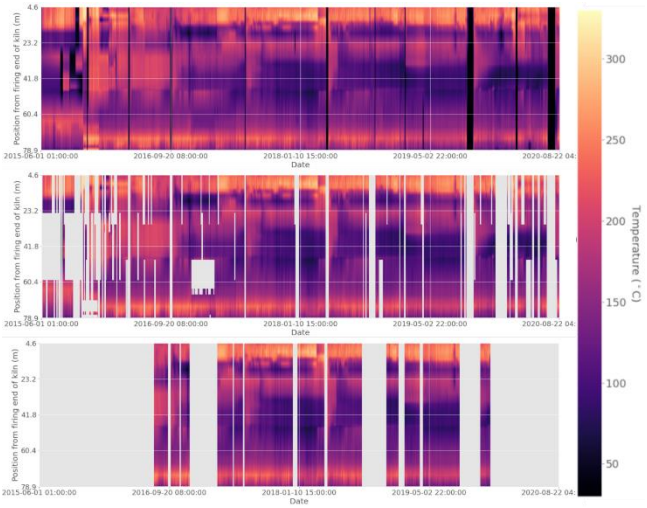

Figure 10. Top: raw KST data from five years of operation. **Middle:** removing invalid data from shutdowns and sensor failures. **Bottom:** Exracting extended periods of clean data for analysis.

Consider the period around 17-11-03 from Figure 7 which shows two high growth days followed by one decay day. To validate these growth and decay events we observe the raw thermal camera images (focusing on measurement area G) and compare the forecast to the measured temperature as shown in Figure 11. The growth indication on 17-11-01 is considered a true positive (TP) given the clear growth from the day prior. For similar reasons the decay indication on 17-11-03 is also considered a TP. However, the growth indication on 17-11-02 is not as certain. The temperature trends indicate potential growth in the first half of the day, but this is not clear from the thermal camera images which are only available every four hours.

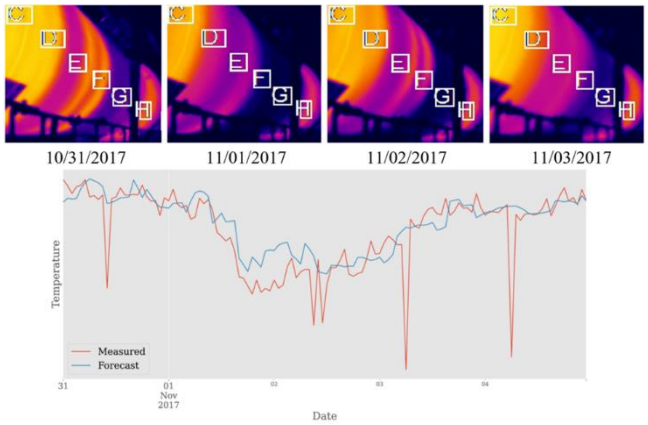

Figure 11. Validating ring formation indications with raw thermal camera images (top) and forecast results (bottom).

A similar manual validation procedure is performed for each of the 75 flagged days. In binary classification terms we are performing two separate binary classifications, i.e., one for ring growth and one for ring decay. The flagged days represent positive events, and the validation of these days is performed to determine the precision of each indicator, i.e., the ratio of TP to all positive events. Table 1 shows the results of the preliminary validation of the ring indicator. To address events with insufficient evidence a second binary label is applied to

each event, i.e., whether the validation assignment is certain. As Table 1 shows, the precision for the growth indicator is 68.2% but only 31.8% of validation labels are considered certain. The results for ring decay are slightly better with a precision of 87.5% and a certainty of 42.5%.

Table 1: Validating growth and decay indications for precision.

Indication	Precision	Certainty
Growth	68.2%	31.8%
Decay	87.5%	42.5%

The major sources of uncertainty are insufficient raw data (e.g., thermal images are too infrequent) and rotational aliasing. Rotational aliasing was discovered as a direct result of the manual validation procedure, and it results in the high frequency KST variations demonstrated in Figure 12. It occurs because the KST measurements are taken as snapshots every minute while the kiln rotates at a speed of approximately 1 rpm, i.e., the KST data does not meet the Nyquist rate [16]. Aliasing causes averaged KST measurements that are not representative of the entire circumference of the kiln. When there is non-uniform build-up of ring material along the circumference the aliasing can cause biased measurements which can result in the high frequency temperature variations demonstrated in Figure 12. This can in turn lead to false positives and high uncertainty of ring indications.

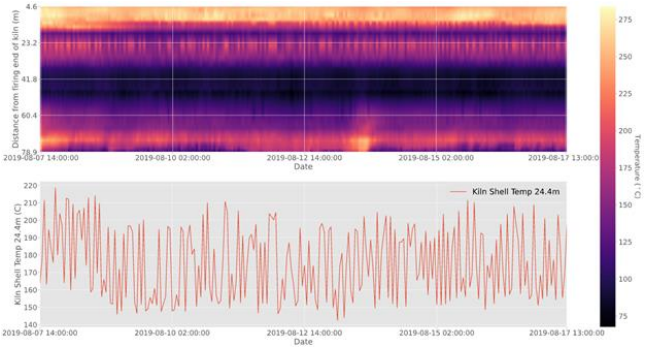

Figure 12. High frequency KST variations changing over 50°C per hour are suspected to be a result of rotational aliasing.

Given this untenable degree of uncertainty, improvements are required to proceed with ring indicator development. One such improvement is enhanced KST measurements to address aliasing. Instead of using 24 measurement areas to collect KST data, a continuous profile line like that shown in Figure 4 is used to collect temperature readings at every pixel. Moreover, instead of taking snapshots every minute, snapshots are now taken every five seconds. These higher frequency snapshots are then averaged into a KST measurement that is more representative of the entire kiln circumference. The plot on the left side of Figure 13 shows the correlation coefficient for each of the profile line positions surrounding the 18 m measurement area. A maximum correlation coefficient of 0.972 is obtained at x-coordinate 325. The plot on the right side of Figure 13 shows the comparison of the measurement area data (red) with the profile line data (blue) which demonstrates the successfully reduced high frequency variability, especially after 2021-08-21.

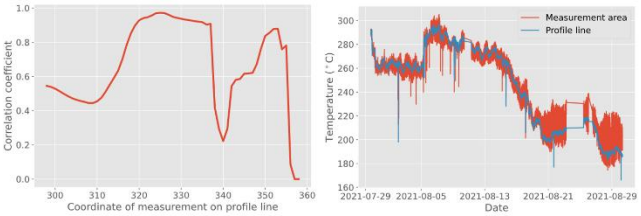

Figure 13. Left: the correlation coefficient between KST data from a measurement area and KST data from various profile line positions denoted by their x-coordinate. **Right:** profile line data with the highest correlation (blue) is plotted with measurement area data (red) to demonstrate improved noise reduction.

Preliminary Insights on Diagnosis

Without a validated ring formation indicator, we are unable to provide rigorous quantitative results on ring diagnosis. However, during this work a great deal of exploratory analysis was conducted whereby we manually diagnose individual ring events. Figure 14 shows an example where the interactive process visualization tool is used to discover mud solids content as a potential cause of ring formation. Given the fact that rings can form gradually over a matter of months, diagnosing a root cause can be very difficult. In addition to mud solids content, other variables of interest are alkali content in the mud (e.g., white liquor clarifier performance), operational instability (e.g., sheet drops), and unmeasured variables such as the amount of dust in the kiln.

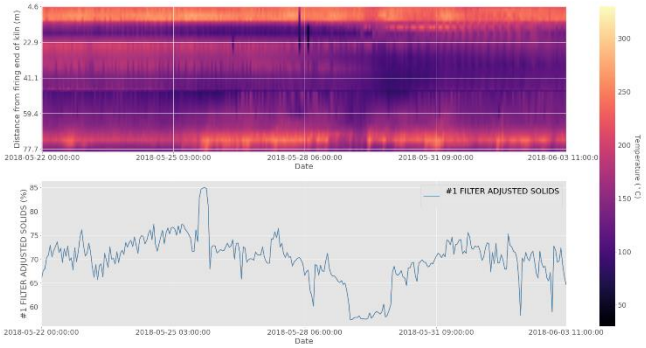

Figure 14. Sustained drop in mud solids content after 2018-05-28 is suspected to cause a mid-kiln ring that persists for weeks.

CONCLUSIONS AND FUTURE WORK

This paper presents our work on detecting and diagnosing ring growth in a rotary lime kiln. A novel approach to visualizing the KST data was developed to enhance our investigation. Although the precision of the proposed ring indicator is fair, the resources available for manual validation are insufficient to be certain. Rotational aliasing was discovered and addressed with an improved KST measurement strategy. Future work will involve another round of manual validation with high frequency data and improved measurements. Finally, future work will leverage the validated indicator to generate quantitative insights into ring diagnosis.

ACKNOWLEDGEMENTS

The authors thank Spartan Controls, the National Science and Engineering Research Council of Canada, and the Izaak Walton Killam Memorial Fund for funding this research.

REFERENCES

1. Russell EL, Chiang LH, Braatz RD Fault detection in industrial processes using canonical variate analysis and dynamic principal component analysis. *Chemometrics and intelligent laboratory systems* 51:81-93 (2000)
2. Spyridon P, Boutalis YS. Generative adversarial networks for unsupervised fault detection. *In 2018 European Control Conference (ECC)* (pp. 691-696). IEEE (2018)
3. Gorog JP, Leary W. Ring removal in rotary kilns used by the pulp and paper industry. *TAPPI J* 15:205-213 (2016)
4. Barham D, Tran HN. An overview of ring formation in lime kilns. *TAPPI Proceedings, 1990 Pulping Conference*, (1990)
5. Tran H, Mao X, Barham D. Mechanisms of ring formation in lime kilns. *J Pulp Paper Sci* 19:J167 (1993)
6. Ribeiro B, Costa E, Dourado A. Lime kiln fault detection and diagnosis by neural networks. *Artificial Neural Nets and Genetic Algorithms* (pp. 112-115). Springer, Vienna (1995).
7. Rippon L, Hirtz B, Sheehan C, Reinheimer T, Loewen P, Gopaluni B. Visualization of multiscale ring formation in a rotary kiln. *Nordic Pulp & Paper Research J.* AOP (2021).
8. Bogdanski BE. The rise and fall of the Canadian pulp and paper sector. *The Forestry Chronicle*, 90:785-793 (2014)
9. Smook GA, Kocurek MJ. Handbook for pulp & paper technologists. *Canadian Pulp and Paper Association* (1982).
10. Dernegård H, Brelid H, Theliander H. Characterization of a dusting lime kiln–A mill study. *Nordic Pulp & Paper Research Journal* 32:25-34 (2017)
11. Natural Resources Canada Office of Energy Efficiency. Benchmarking energy use in Canadian pulp and paper mills. *Ottawa – Ontario: Natural Resources Canada* (2008)
12. Hirtz B, Marshman D, Sheehan C. Kiln Infra-Red Cameras for Abnormal Situation Detection and Residual Carbonate Control. *JFOR: J Sci Technol For Prod Process*, 6:28-36 (2017)
13. Tran H. Lime kiln chemistry and effects on kiln operations. *Pulp & Paper Centre and Department of Chemical Engineering and Applied Chemistry, University of Toronto*, Toronto, Canada (2007)
14. Lindblom J, Theliander H. The Influence of Carbon Dioxide on Ring and Ball Formation in a Pilot-Scale Rotary Kiln. *KONA Powder Particle J*, 19:109-117 (2001)
15. Lv F, Wen C, Bao Z, Liu M. Fault diagnosis based on deep learning. *In 2016 American control conference (ACC)* (pp. 6851-6856). IEEE (2016)
16. Shannon CE Communication in the presence of noise. *Proceedings of the IRE*, 37:10-21 (1949)

This conference proceeding has not been peer reviewed.